Sum rules and convex optimization

Daniel Sjöberg

Department of Electrical and Information Technology, Lund University, Sweden

SSF Workshop, Lund, January 15, 2015

Outline

1. **Introduction**
2. **Sum rules**
3. **Representation of positive real functions**
4. **Convex optimization**
5. **Conclusions**

Outline

1. **Introduction**
2. **Sum rules**
3. **Representation of positive real functions**
4. **Convex optimization**
5. **Conclusions**

Motivation

Passive systems can be represented by Herglotz functions $h(\omega)$ (or positive real functions $p(s)$, where $s = -\mathrm{i}\omega = \mathrm{j}\omega$), for instance

- Refractive index: $h(\omega) = \omega n(\omega)$, $p(s) = sn(s)$.
- Permittivity: $h(\omega) = \omega\epsilon(\omega)$, $p(s) = s\epsilon(s)$.
- Impedance: $h(\omega) = X(\omega) + \mathrm{i}R(\omega)$, $p(s) = R(s) + \mathrm{j}X(s)$.

It is often interesting to consider non-standard values, like $n \approx -1$ or $n \approx 0$.

- Herglotz functions: 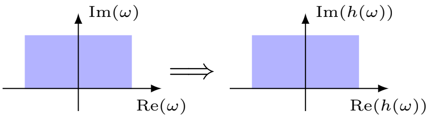

- Positive real functions: 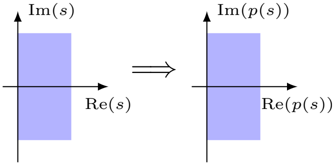

Example: negative refractive index

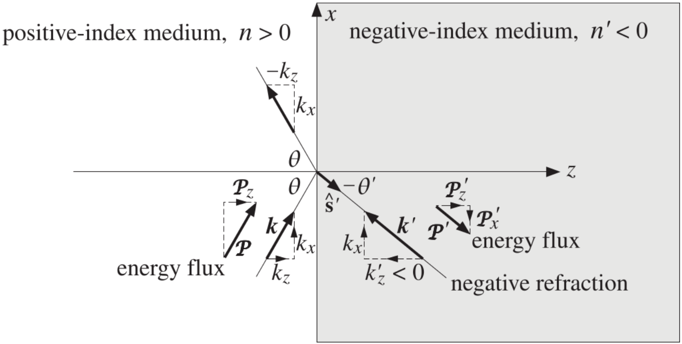

- Snel's law $n \sin\theta = n' \sin\theta'$ and $n' = -n$ implies $\theta' = -\theta$.
- A slab of $n' = -1$ has been discussed as a "perfect lens".

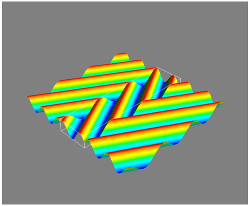

Consequences of deviations from design value

Evanescent waves ($k_x > k_0$) are amplified in a negative index slab.

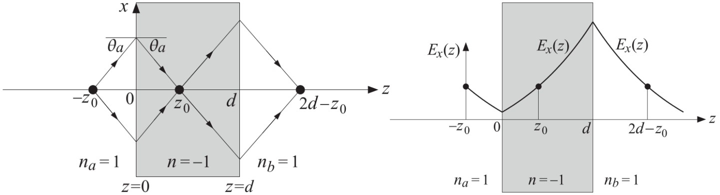

Consequences of deviations from design value

Evanescent waves ($k_x > k_0$) are amplified in a negative index slab.

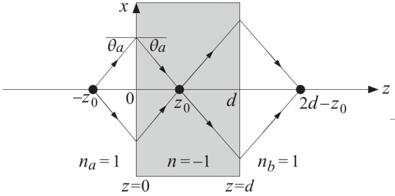

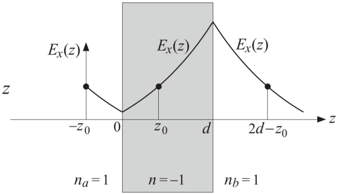

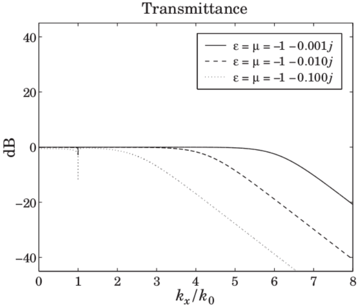

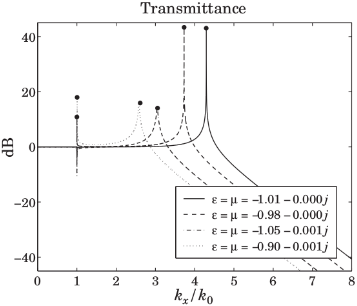

Figures from Orfanidis, *Electromagnetic Waves and Antennas*.

Outline

Asymptotics and sum rules

With knowledge of the low and high frequency asymptotics of a Herglotz function,

$$h(\omega) = \begin{cases} a_{-1}\omega^{-1} + a_1\omega + \ldots + a_{2N_0-1}\omega^{2N_0-1} + o(\omega^{2N_0-1}) & \text{as } \omega \hat{\to} 0 \\ b_1\omega + b_{-1}\omega^{-1} + \ldots + b_{1-2N_\infty}\omega^{1-2N_\infty} + o(\omega^{1-2N_\infty}) & \text{as } \omega \hat{\to} \infty \end{cases}$$

the following sum rules can be derived

$$\frac{2}{\pi}\int_{0+}^{\infty} \frac{\operatorname{Im} h(\omega)}{\omega^{2n}}\,\mathrm{d}\omega = a_{2n-1} - b_{2n-1},$$

for $n = 1 - N_\infty, \ldots, N_0$.

When the integral and the asymptotics can be given physical interpretation, the sum rule represents a physical bound.

Physical bounds for bounded regions

Some examples of physical bounds for electromagnetic interaction developed in Lund.

- JPA 2007: Extinction cross section for finite scatterers

$$\int_0^\infty \sigma_{\mathrm{ext}}(\lambda)\,\mathrm{d}\lambda = \pi^2 \hat{\boldsymbol{e}} \cdot \boldsymbol{\gamma} \cdot \hat{\boldsymbol{e}}$$

- TAP 2009: Directivity and Q for antennas (best paper 2009)

$$\frac{D}{Q} \leq \eta \frac{4\pi^2}{\lambda_0^3} \hat{\boldsymbol{e}} \cdot \boldsymbol{\gamma} \cdot \hat{\boldsymbol{e}}$$

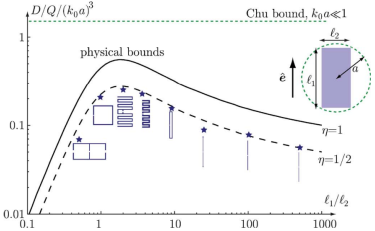

Physical bounds for surfaces and materials

In all cases the bandwidth is $B = (\lambda_2 - \lambda_1)/\lambda_0$.

- EPL 2009/10: Band stop for low pass films ($|T| < T_0$):

$$B \ln \frac{1}{T_0} \leq \frac{\pi^2}{2A\lambda_0} \hat{\boldsymbol{e}} \cdot \boldsymbol{\gamma} \cdot \hat{\boldsymbol{e}}$$

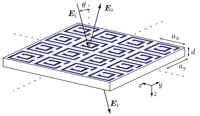

- NJP 2010: Metamaterials designed for $\epsilon \approx \epsilon_m < \epsilon_\infty$ ($\epsilon_m = -1$):

$$\max_{\omega \in \mathcal{B}} |\epsilon(\omega) - \epsilon_m| \geq \frac{B/2}{1 + B/2}(\epsilon_\infty - \epsilon_m)$$

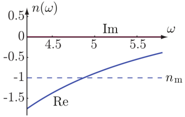

- TAP 2011: Reflection from high impedance surfaces ($|Z| > Z_0/\Delta$):

$$\frac{B}{\Delta} \leq \frac{4\pi}{\lambda_0}\left(d + \frac{\gamma}{2A}\right)$$

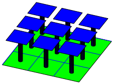

Outline

Representation of positive real functions

An impedance or admittance is a positive real function, that is,

- $P(s)$ is an analytic mapping of the right half plane to itself, with symmetry $P(s) = P^*(s^*)$.

There is a general representation formula for positive real functions

$$P(s) = sC + \frac{1}{\pi}\int_{-\infty}^{\infty} \frac{s\,\mathrm{Re}\{P(\mathrm{j}\xi)\}}{\xi^2 + s^2}\,\mathrm{d}\xi$$

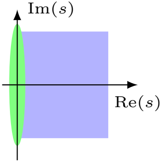

On the frequency axis $s = \mathrm{j}\omega$ the integral is

$$P(\mathrm{j}\omega) = \mathrm{j}\omega C + \frac{1}{\pi}\int_{-\infty}^{\infty} \frac{\mathrm{j}\omega\,\mathrm{Re}\{P(\mathrm{j}\xi)\}}{\xi^2 - \omega^2}\,\mathrm{d}\xi = \mathrm{j}\omega C + \frac{1}{\mathrm{j}\pi}\int_{-\infty}^{\infty} \frac{\mathrm{Re}\{P(\mathrm{j}\xi)\}}{\omega - \xi}\,\mathrm{d}\xi$$

which shows the real and imaginary parts are related by the Hilbert transform. However, the evaluation on the frequency axis requires close attention to poles, and $P(\mathrm{j}\omega)$ is not necessarily in L^2.

Some Hilbert transform pairs

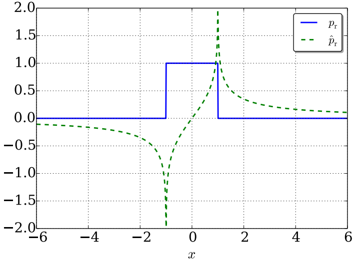

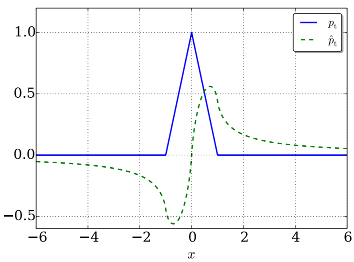

Rectangular pulse

Triangular pulse

$$p(x) = \begin{cases} 1 & |x| < 1 \\ 0 & |x| > 1 \end{cases}$$

$$[\mathcal{H}p](x) = \frac{1}{\pi} \ln \left| \frac{x+1}{x-1} \right|$$

$$p(x) = \begin{cases} 1 - |x|, & |x| \le 1 \\ 0, & |x| > 1 \end{cases}$$

$$[\mathcal{H}p](x) = -\frac{1}{\pi} \left(x \ln \left| \frac{x^2}{x^2 - 1} \right| + \ln \left| \frac{x-1}{x+1} \right| \right)$$

There's plenty more where that came from!

Appendix 1 of Frederick W. King's book on Hilbert transforms has 80 pages of transform pairs.

Number	$f(x)$	$\frac{1}{\pi} P \int_{-\infty}^{\infty} \frac{f(s)\,ds}{x-s}$
(2.24)	$\dfrac{ax^3+bx^2+cx+d}{(1+x^4)}$	$[(x^4+1)\sqrt{2}]^{-1}\{x^3(b+d)-x^2(a-c)-x(b-d)-a-c\}$
(2.25)	$\dfrac{ax^3+bx^2+cx+d}{(1+x^2)^2}$	$[2(1+x^2)^2]^{-1}\{x^3(b+d)+x^2(c-3a)+x(3d-b)-a-c\}$
(2.26)	$\dfrac{x(1-x^2)}{x^4+(a^2-2)x^2+1}, \quad a>0$	$\dfrac{ax^2}{x^4+(a^2-2)x^2+1}$
(2.27)	$\dfrac{1}{(x^6+a^6)}, \quad a>0$	$\dfrac{x(2x^4+a^2x^2+2a^4)}{3a^5(x^6+a^6)}$
(2.28)	$\dfrac{1}{(x^2+a^2)^3}, \quad a>0$	$\dfrac{x(3x^4+10a^2x^2+15a^4)}{8a^5(x^2+a^2)^3}$
(2.29)	$\dfrac{1}{(x^4+a^4)(x^2+b^2)}, \quad a>0, \; b>0$	$[2a^3b(a^4+b^4)(x^4+a^4)(x^2+b^2)]^{-1}\{a^2(2a^5+\sqrt{(2)}\,a^2b^3+\sqrt{(2)}\,b^5)x + b\sqrt{(2)}\,(a^4+b^4)x^3+(2a^3-\sqrt{(2)}\,a^2b+\sqrt{(2)}\,b^3)x^5\}$
(2.30)	$\dfrac{x}{(x^4+1)(x^2+1)},$	$\dfrac{\sqrt{2}\,x^2(x^2+1)-(x^4+1)}{2(x^2+1)(x^4+1)}$
(2.31)	$[(x^2+a^2)(x^2+b^2)(x^2+c^2)]^{-1},$ $a>0, \; b>0, \; c>0$	$[abc(a+b)(b+c)(c+a)(x^2+a^2)(x^2+b^2)(x^2+c^2)]^{-1}x[(a+b+c)x^4 + (a^3+b^3+c^3+a^2b+a^2c+b^2a+b^2c+c^2a+c^2b+abc)x^2+a^3b^2 + a^3c^2+b^3a^2+b^3c^2+c^3a^2+c^3b^2+a^3bc+b^3ac+c^3ab+2(a^2b^2c + a^2c^2b+b^2c^2a)]$
(2.32)	$\dfrac{x}{(x^6+a^6)}, \quad a>0$	$\dfrac{x^4+2a^2x^2-2a^4}{3a^3(x^6+a^6)}$
(2.33)	$\dfrac{x}{(x^2+a^2)^3}, \quad a>0$	$\dfrac{x^4+6a^2x^2-3a^4}{8a^3(x^2+a^2)^3}$

461

Expansion of causal signals

A causal signal $F(\omega) = F_{\mathrm{r}}(\omega) + \mathrm{j}F_{\mathrm{i}}(\omega)$ satisfies $F_{\mathrm{i}} = -\mathcal{H}F_{\mathrm{r}}$. By expanding the real part in pulse functions, the imaginary part is also given:

$$F_{\mathrm{r}}(\omega) = \sum_{n=-N}^{N} x_n p(\omega/\Delta\omega - n), \quad F_{\mathrm{i}}(\omega) = -\sum_{n=-N}^{N} x_n [\mathcal{H}p](\omega/\Delta\omega - n)$$

The x_n are pointwise samples of the real part, $x_n = F_{\mathrm{r}}(n\Delta\omega)$.

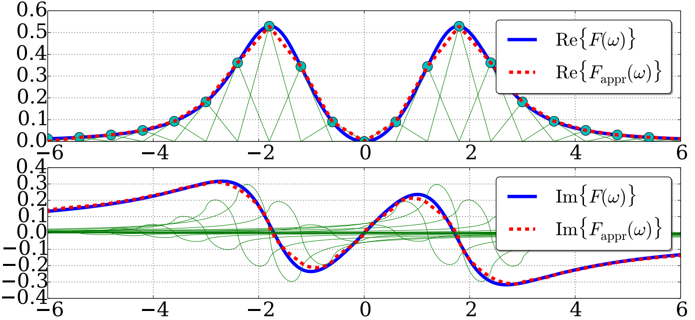

Representation of causal systems

Using an expansion in Hilbert transform pairs together with a constant conductance and poles at infinity and zero (capacitance and inductance), we can represent an admittance function $Y(\omega) = G(\omega) + \mathrm{j}B(\omega)$ as

$$G(\omega) = G_0 + \sum_{n=0}^{N} x_n \left\{ p(\omega/\Delta\omega - n) + p(\omega/\Delta\omega + n) \right\}$$

$$B(\omega) = C\omega - \frac{1}{L\omega} - \sum_{n=0}^{N} x_n \left\{ [\mathcal{H}p](\omega/\Delta\omega - n) + [\mathcal{H}p](\omega/\Delta\omega + n) \right\}$$

where we used the symmetry $G(\omega) = G(-\omega)$, and $\Delta\omega$ is the spacing. This gives us a parameterized representation formula $Y(\omega; x)$, where $x = (G_0, C, L^{-1}, \{x_n\}_{n=0}^{N})$.

Note that using L^{-1} as parameter makes $Y(\omega; x)$ linear in x.

Outline

Convex optimization

Using $Y(\omega;x)$, we can set up the convex optimization problem (convex functional and convex constraints)

$$\begin{aligned} &\text{minimize} && \|Y(\omega;x) - Y_{\mathrm{t}}(\omega)\| \\ &\text{subject to} && G_0, C, L^{-1} \geq 0 \\ & && x_n \geq 0, \quad n = 0, 1, \ldots, N \end{aligned}$$

for any target admittance $Y_{\mathrm{t}}(\omega)$. More specific constraints can be made on G_0, C, and L^{-1} when they can be interpreted physically.

Very powerful methods exist for convex optimization. Once the problem is formulated as above, it can be considered as solved.

In the following, the optimization frequencies and expansion constants are scaled to a center frequency, $\omega \to \omega/\omega_0$, $C \to C\omega_0$ etc. The design band in the examples is $\omega/\omega_0 \in \Omega = [0.75, 1.25]$.

Metamaterials, negative refractive index

- Refractive index $n(\omega) = n'(\omega) - \mathrm{j}n''(\omega) \Rightarrow Y(\omega) = \mathrm{j}\omega n(\omega)$.
- Target admittance: $Y_{\mathrm{t}}(\omega) = -\mathrm{j}\omega$ for $\omega \in \Omega$.
- $n(0)$ either finite or $\sim 1/\sqrt{\omega}$ implies $Y(0) = 0 \Rightarrow L^{-1} = 0$.
- $C = n_\infty \geq 1$ due to special relativity.

Metamaterials, negative refractive index

- Refractive index $n(\omega) = n'(\omega) - \mathrm{j}n''(\omega) \Rightarrow Y(\omega) = \mathrm{j}\omega n(\omega)$.
- Target admittance: $Y_{\mathrm{t}}(\omega) = -\mathrm{j}\omega$ for $\omega \in \Omega$.
- $n(0)$ either finite or $\sim 1/\sqrt{\omega}$ implies $Y(0) = 0$ $\Rightarrow L^{-1} = 0$.
- $C = n_\infty \geq 1$ due to special relativity.

$$\begin{array}{ll} \text{minimize} & \|Y(\omega; x) + \mathrm{j}\omega\|_{\infty,\Omega} \\ \text{subject to} & Y(0; x) = G_0 + 2x_0 = 0 \\ & G_0, x_n \geq 0 \\ & L^{-1} = 0 \\ & C \geq 1 \\ & \|G(\omega; x)/\omega\|_{\infty,\Omega} \leq n''_{\max} \end{array}$$

Metamaterials, negative refractive index

- Refractive index $n(\omega) = n'(\omega) - \mathrm{j}n''(\omega) \Rightarrow Y(\omega) = \mathrm{j}\omega n(\omega)$.
- Target admittance: $\boxed{Y_{\mathrm{t}}(\omega) = -\mathrm{j}\omega}$ for $\omega \in \Omega$.
- $n(0)$ either finite or $\sim 1/\sqrt{\omega}$ implies $\boxed{Y(0) = 0} \Rightarrow L^{-1} = 0$.
- $C = n_\infty \geq 1$ due to special relativity.

$$
\begin{aligned}
\text{minimize} \quad & \|Y(\omega;x) + \mathrm{j}\omega\|_{\infty,\Omega} \\
\text{subject to} \quad & Y(0;x) = G_0 + 2x_0 = 0 \\
& G_0, x_n \geq 0 \\
& L^{-1} = 0 \\
& C \geq 1 \\
& \|G(\omega;x)/\omega\|_{\infty,\Omega} \leq n''_{\max}
\end{aligned}
$$

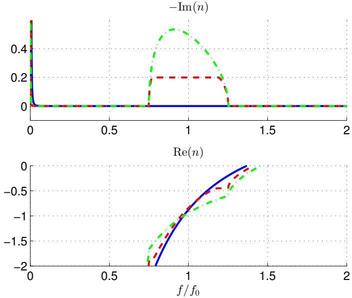

- Solid blue line: lossless case ($n''_{\max} = 0$).
- Dashed red line: constrained losses ($n''_{\max} = 0.2$).
- Dash-dotted green line: unconstrained losses ($n''_{\max} = 1$).

Acceptable loss levels can be specified.

High impedance surfaces, PEC backing

- High impedance $\Leftrightarrow$ low admittance $\Rightarrow$ $\boxed{Y_{\mathrm{t}}(\omega) = 0}$ for $\omega \in \Omega$.
- PEC backing nonmagnetic $\Rightarrow r = -1 + 2\mathrm{j}kd + \mathrm{O}((kd)^2)$
  $\Rightarrow \boxed{Y = \frac{1-r}{1+r} = -\mathrm{j}/(kd) + \mathrm{O}(1)} \Rightarrow L = 2\pi d/\lambda_0$.

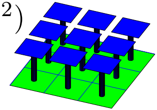

- For a maximal allowed d/λ_0, we have $L^{-1} \geq q$.

High impedance surfaces, PEC backing

- High impedance $\Leftrightarrow$ low admittance $\Rightarrow$ $\boxed{Y_{\mathrm{t}}(\omega) = 0}$ for $\omega \in \Omega$.
- PEC backing nonmagnetic $\Rightarrow r = -1 + 2\mathrm{j}kd + \mathrm{O}((kd)^2)$
  $\Rightarrow \boxed{Y = \frac{1-r}{1+r} = -\mathrm{j}/(kd) + \mathrm{O}(1)} \Rightarrow L = 2\pi d/\lambda_0$.

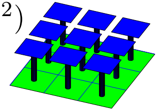

- For a maximal allowed d/λ_0, we have $L^{-1} \geq q$.

$$
\begin{array}{ll}
\text{minimize} & \|Y(\omega; x)\|_{\infty,\Omega} \\
\text{subject to} & G_0, C, x_n \geq 0 \\
 & L^{-1} \geq q \\
 & \|G(\omega; x)\|_{\infty,\Omega} \leq G_{\max}
\end{array}
$$

High impedance surfaces, PEC backing

- High impedance $\Leftrightarrow$ low admittance $\Rightarrow$ $\boxed{Y_\mathrm{t}(\omega) = 0}$ for $\omega \in \Omega$.
- PEC backing nonmagnetic $\Rightarrow r = -1 + 2\mathrm{j}kd + \mathrm{O}((kd)^2)$
  $\Rightarrow \boxed{Y = \frac{1-r}{1+r} = -\mathrm{j}/(kd) + \mathrm{O}(1)} \Rightarrow L = 2\pi d/\lambda_0$.
- For a maximal allowed d/λ_0, we have $L^{-1} \geq q$.

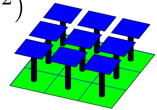

$$\begin{aligned} &\text{minimize} && \|Y(\omega;x)\|_{\infty,\Omega} \\ &\text{subject to} && G_0, C, x_n \geq 0 \\ &&& L^{-1} \geq 0.1 \\ &&& \|G(\omega;x)\|_{\infty,\Omega} \leq G_{\max} \end{aligned}$$

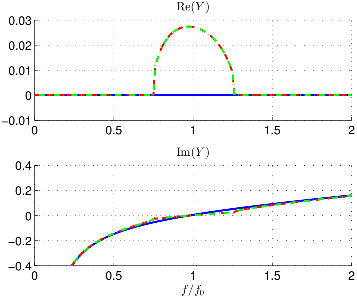

- Solid blue line: lossless case ($G_{\max} = 0$).
- Dashed red line: constrained losses ($G_{\max} = 0.2$).
- Dash-dotted green line: unconstrained losses ($G_{\max} = 10$).

High impedance surfaces, PEC backing

- High impedance $\Leftrightarrow$ low admittance $\Rightarrow$ $\boxed{Y_{\mathrm{t}}(\omega) = 0}$ for $\omega \in \Omega$.
- PEC backing nonmagnetic $\Rightarrow r = -1 + 2\mathrm{j}kd + \mathrm{O}((kd)^2)$
  $\Rightarrow \boxed{Y = \frac{1-r}{1+r} = -\mathrm{j}/(kd) + \mathrm{O}(1)} \Rightarrow L = 2\pi d/\lambda_0$.

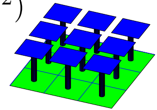

- For a maximal allowed d/λ_0, we have $L^{-1} \geq q$.

$$
\begin{array}{ll}
\text{minimize} & \|Y(\omega;x)\|_{\infty,\Omega} \\
\text{subject to} & G_0, C, x_n \geq 0 \\
& L^{-1} \geq 1 \\
& \|G(\omega;x)\|_{\infty,\Omega} \leq G_{\max}
\end{array}
$$

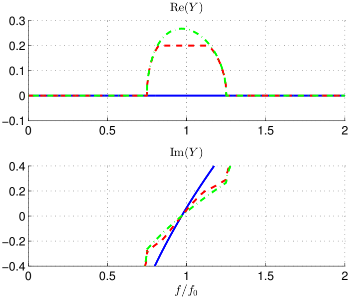

- Solid blue line: lossless case ($G_{\max} = 0$).
- Dashed red line: constrained losses ($G_{\max} = 0.2$).
- Dash-dotted green line: unconstrained losses ($G_{\max} = 10$).

High impedance surfaces, PEC backing

- High impedance $\Leftrightarrow$ low admittance $\Rightarrow$ $\boxed{Y_{\mathrm{t}}(\omega) = 0}$ for $\omega \in \Omega$.
- PEC backing nonmagnetic $\Rightarrow r = -1 + 2\mathrm{j}kd + \mathrm{O}((kd)^2)$
  $\Rightarrow \boxed{Y = \frac{1-r}{1+r} = -\mathrm{j}/(kd) + \mathrm{O}(1)} \Rightarrow L = 2\pi d/\lambda_0$.
- For a maximal allowed d/λ_0, we have $L^{-1} \geq q$.

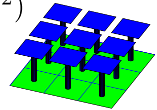

$$
\begin{array}{ll}
\text{minimize} & \|Y(\omega;x)\|_{\infty,\Omega} \\
\text{subject to} & G_0, C, x_n \geq 0 \\
& L^{-1} \geq 10 \\
& \|G(\omega;x)\|_{\infty,\Omega} \leq G_{\max}
\end{array}
$$

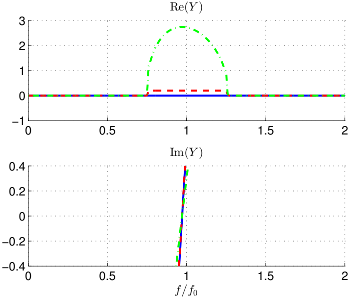

- Solid blue line: lossless case ($G_{\max} = 0$).
- Dashed red line: constrained losses ($G_{\max} = 0.2$).
- Dash-dotted green line: unconstrained losses ($G_{\max} = 10$).

High impedance surfaces, PEC backing

- High impedance $\Leftrightarrow$ low admittance $\Rightarrow$ $\boxed{Y_{\mathrm{t}}(\omega) = 0}$ for $\omega \in \Omega$.
- PEC backing nonmagnetic $\Rightarrow r = -1 + 2\mathrm{j}kd + \mathrm{O}((kd)^2)$
  $\Rightarrow \boxed{Y = \frac{1-r}{1+r} = -\mathrm{j}/(kd) + \mathrm{O}(1)} \Rightarrow L = 2\pi d/\lambda_0$.
- For a maximal allowed d/λ_0, we have $L^{-1} \geq q$.

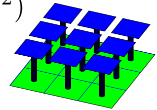

$$
\begin{array}{ll}
\text{minimize} & \|Y(\omega; x)\|_{\infty,\Omega} \\
\text{subject to} & G_0, C, x_n \geq 0 \\
& L^{-1} \geq 1 \\
& \|G(\omega; x)\|_{\infty,\Omega} \leq G_{\max}
\end{array}
$$

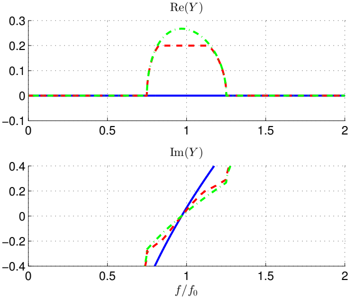

- Solid blue line: lossless case ($G_{\max} = 0$).
- Dashed red line: constrained losses ($G_{\max} = 0.2$).
- Dash-dotted green line: unconstrained losses ($G_{\max} = 10$).

Maximal thickness and acceptable loss level can be specified.

Outline

Conclusions

- Sum rules can be used to derive physical bounds.
- A parameterized representation based on Hilbert transform pairs can be used for positive real functions.
- Convex optimization was applied to characterize the behavior in circumstances unavailable for sum rule methods.
- The convex optimization approach allows significant freedom in the problem formulation.